Methacrylated Self-Organizing 2,3,4-Tris(alkoxy)benzenesulfonate: A New Concept Toward Ion-Selective Membranes

Xiaomin Zhu,[†] Maxim A. Scherbina,[‡] Artem V. Bakirov,[‡] Blazej Gorzolnik,[†] Sergei N. Chvalun,[‡] Uwe Beginn,*[,†] and Martin Möller*[,†]

DWI an der RWTH Aachen e.V. and Institute of Technical and Macromolecular Chemistry at RWTH Aachen, Pauwelsstrasse 8, D-52056 Aachen, Germany, and Karpov Institute of Physical Chemistry, Vorontsovo Pole 10, 103064 Moscow, Russia

Received February 7, 2006. Revised Manuscript Received June 23, 2006

The synthesis of 2,3,4-tris(11′-methacryloylundecyl-1′-oxy)benzenesulfonic acid and its sodium salt is described. The thermal behavior of the compounds was investigated by a combination of polarizing optical microscopy and differential scanning calorimetry. The sodium salt forms a hexagonal columnar disordered phase (Col_{hd}), whereas the acid is a crystalline compound. X-ray scattering analysis and force-field-based molecular modeling provided insight into the molecular arrangement in the mesophase. The sulfonate groups are confined in the center of the columns, preforming a potential ion-transport channel along the column axis. Thin films of the sodium sulfonate were photopolymerized in the mesomorphous state, yielding free-standing foils with embedded potential ion channels.

Introduction

Biological membranes establish the fundamental barrier between the interior and exterior of cells; they contain highly selective channels, consisting of reversibly self-organized aggregates of functional proteins. These channels regulate the permeation of nutrients and osmolytes to maintain viability.[1] It is still a principal challenge to model such behavior and to prepare synthetic functional membranes, mimicking the characteristics of native protein-assisted ion transport. The availability of such membranes would induce a revolutionary change in industrial and laboratory practice, as energy- and labor-intensive purification methods could be replaced by isothermal membrane processes.[2] Moreover, highly selective membranes would also simplify numerous separation tasks or detection problems in the fields of biochemical, medical, or even environmental analytical technology.[3]

An example of industrially applied synthetic ion-selective membranes is perfluorinated ionomer membranes (Nafion). In addition to their good mechanical properties and superior chemical inertness, these ionomers provide an unusual degree of permeability selectivity in favor of cations over anions. This selectivity exceeds the well-understood Donnan permselectivity, based on differences in the equilibrium sorption of counterions and co-ions in an ion-exchanging medium.[4] The persistence of permselectivity beyond the Donnan limit has been referred to as "superselectivity".[5] Among others, a "cluster-network" model was proposed to describe the structure of these ionomers.[6] The polymeric ions and the absorbed water molecules separate from the fluorocarbon matrix into domains, approximately 4−5 nm in diameter, connected by short narrow channels ($\Phi \approx 1$ nm). The fixed charges are embedded in the aqueous phase, close to the water/fluorocarbon interface. Although the overall charge density of the membrane is comparable to that of other ion-exchange membranes[4] (1−10 mequiv/cm^3), the local concentration of the fixed charges in the ion clusters far exceeds this value. Thus, co-ions are strongly rejected even at elevated source phase concentrations. Because the diameters of the intercluster channels are below the Debye length of the permeating ions, Nafion membranes also exhibit high cation−cation selectivity, i.e., larger, more hydrophobic ions exhibit significantly lower transport rates than small hydrophilic ions.[7] It is a severe disadvantage of perfluorinated ionomer system that the content of the cluster phase cannot be arbitrarily increased, because the ionomers become water soluble when a certain sulfonate content is exceeded.[8]

* To whom correspondence should be addressed. PD Dr. Uwe Beginn: tel., +49-241-80-23341; fax, +49-241-80-23301; e-mail, beginn@dwi.rwth-aachen.de. Prof. Dr. Martin Möller: tel., +49-241-80-23302; fax, +49-241-80-23301; e-mail, moeller@dwi.rwth-aachen.de.

[†] DWI and Institute of Technical and Macromolecular Chemistry at RWTH Aachen.

[‡] Karpov Institute of Physical Chemistry.

(1) Alberts, B.; Bray, D.; Lewis, J.; Raff, M.; Roberts, K.; Watson, J. D. *The Molecular Biology of the Cell*, 3rd ed.; Garland Publishers: New York, 1994.

(2) (a) Peinemann, K. V., Nunes, S. P., Eds. *Membrane Technology in the Chemical Industry*; Wiley-VCH: Weinheim, Germany, 2006, (b) Hoffman, E. J. *Membrane Separations Technology*; Gulf Professional Publishing/Elsevier Science: Amsterdam, 2003, (c) Feng, X.; Huang, R. Y. M. *Ind. Eng. Chem. Res.* **1997**, *36*, 1048, (d) Baker, R. W. In *Membrane Separation Systems—A Research & Development Needs Assessment*; Baker, R. W., Cussler, E. L., Eykamp, W., Koros, W. J., Riley, R. L., Strathmann, H., Eds.; U.S. Department of Energy: Washington, DC, 1990; Contract No. DE-AC01-88ER30133.

(3) (a) Afonso, C. A. M., Crespo, J. G., Eds. *Green Separation Processes*; Wiley-VCH: Weinheim, Germany, 2005. (b) Pinnau, I., Freeman, B. D., Eds.; *Advanced Materials for Membrane Separations*; ACS Symposium Series 876; American Chemical Society: Washington, DC, 2004. (c) Noble, R. D., Stern A. S., Eds. *Membrane Separation Technology—Principles and Applications*; Elsevier: Amsterdam, 1995.

(4) Helfferich, F. *Ion Exchange*; McGraw-Hill: New York, 1962; Chapter 6.

(5) Reiss, H.; Bassignana, I. C. *J. Membr. Sci.* **1982**, *11*, 219.

(6) (a) Mauritz, K. M.; Moore R. B. *Chem. Rev.* **2004**, *104*, 4535. (b) Hsu, W. Y.; Gierke, T. D. *J. Membr. Sci.* **1983**, *13*, 307.

(7) Robertson, M. A. F.; Yeager, H. L. *Macromolecules* **1996**, *29*, 5166.

10.1021/cm060305y CCC: $33.50
Published on Web 08/26/2006

Herein, we present a new concept for preparing well-defined cylindrical sulfonate ion-transport channels based on the self-assembly of amphiphilic sulfonate molecules. It is expected that functional membranes containing such channels can be used as models to increase the understanding of the peculiarities of the transport phenomena observed with Nafion systems.

As shown in previous work, wedge-shaped molecules bearing polar groups at the tip of the wedge generally tend to form cylindrical superstructures with the polar groups arranged along the cylinder axis.[9] According to this concept, the self-assembled cylinder formation of benzamide,[10] crown ether,[11] and carbohydrate amphiphiles[12] has been demonstrated. Recently, we showed that wedge-shaped sulfonate amphiphiles form supramolecular columns in which the sulfonate groups are stacked parallel to the column axis, forming a potential ion channel.[13] In this work, we describe the synthesis and self-organization properties of sodium 2,3,4-tris(11′-methacryloylundecyl-1′-oxy)benzenesulfonate, a new polymerizable wedge-shaped sulfonate compound. The presence of methacrylate end groups allows a covalent connection of the supramolecular aggregates to polymer matrixes, hence generating solid materials suitable for membrane applications.

Experimental Section

Materials. Pyrogallol (puriss. 99%, Riedel-de Haën), 11-bromo-1-undecanol (98%, Aldrich), sulfuric acid (95−97%, GR for analysis, Merck), methacryloyl chloride (97%, Fluka), triethylamine (p.a. grade, Merck), potassium carbonate (99%, Merck), cyclohexanone (z.S., Merck), 4-(dimethylamino)pyridine (99%, Aldrich), 2,6-di-*tert*-butyl-4-methylphenol (99%, Aldrich), 2,2-dimethoxy-2-phenylacetophenone (99%, Aldrich), and Amberlyst 15 ion-exchange resin (Aldrich) were used as received. Tetrahydrofuran (THF), *n*-hexane, ethyl acetate, chloroform, diethyl ether, sodium sulfate, sodium hydrogen carbonate, and sodium hydroxide were gifts from the "Fonds der Chemischen Industrie". The solvents were purified according to standard procedures.

Techniques. ^{1}H NMR (300 MHz) and ^{13}C NMR (75 MHz) spectra were recorded on a Bruker DPS 300 spectrometer, using tetramethylsilane (TMS) as an internal standard. Thin-layer chromatography (TLC) was performed on Merck KG-60/F254 TLC plates with detection by illumination with UV light (254 nm) or use of iodine vapor. Elemental analysis of **3** was performed in the microanalytical laboratory of the A. N. Nesmeyanov Institute of Organoelement Compounds of the Russian Academy of Sciences; other compounds were analyzed on a Carlo Erba MOD 1106 instrument.

For thermooptical analysis, a Zeiss AXIOSKOP polarizing microscope equipped with a Mettler FP 82 hot stage was used. Differential scanning calorimetry (DSC) measurements were performed using a Netzsch DSC 204 unit. Samples (typical weight, 5 mg) were enclosed in standard Netzsch 25-μL aluminum crucibles. Indium and palmitic acid were used as calibration standards. Heating and cooling rates were 10 K min^{-1}.

Small-angle X-ray scattering (SAXS) data were recorded using a Kratky block camera and Ni-filtered Cu Kα radiation The diverging and receiving slits were 100 and 100 μm wide, respectively, providing high resolution; the half-width of the primary beam was approximately 1.5′ (angular minutes), i.e., 1.8×10^{-3} Å^{-1}. The scattered intensity was measured at angular increments of 0.5′ in the region of the narrow, intense 10 reflection and at 1′ increments over the rest of the measured region. Storage times were about 100−300 s per point, depending on the relative intensity of the peaks. The temperature interval for the temperature attachment was between 20 and (250 ± 1) °C. Oriented fibers for X-ray analysis were prepared by drawing from the melt at temperatures above 60 °C. The X-ray pattern of the oriented fiber was recorded at room temperature using pinhole camera.

Transmission electron microscopy analysis was conducted on a Philips EM10 microscope operating at 100 kV in the bright-field mode. Samples were prepared by microtoming thin sections (thickness ≈ 50 nm as indicated by the interference color) at ambient temperature with a diamond knife (LEITZ) on a Reichert Ultramicrotome. The sections were transferred on copper grids and stained in the gas phase with ruthenium tetroxide, obtained from ruthenium trichloride hydrate in 10 wt % sodium hypochloride solution.

Molecular modeling was performed with MacroModel 8.0,[14] using the MMFF force field in a vacuum. Electrostatic interactions were treated by a distance-dependent dielectric constant. Its value and distance dependences were defined by the force field. The electric charges of the atoms were also taken into account through the force-field definition.[15] The cutoff distances were 0.7 nm for van der Waals interactions, 1.2 nm for electrostatic interactions, and 0.4 nm for hydrogen-bond interactions. Structure optimization was performed by application of the Polak−Ribiere algorithm[16] to start conformations until a final gradient below 0.5 kJ/nm was reached. The structure was refined further by means of the Truncated Newton Conjugate Gradient method[16] until the final gradient was below 0.05 kJ/nm.

Syntheses. *1,2,3-Tris(11′-hydroxyundecyl-1′-oxy)benzene (**1**).* In a 500-mL three-neck round-bottom flask equipped with a nitrogen inlet and a cooler, 3 g (23.8 mmol) of pyrogallol and 20.6 g (82.1 mmol) of 11-bromo-1-undecanol were dissolved in 200 mL of cyclohexanone. To this solution was added 32.88 g (237.9 mmol) anhydrous potassium carbonate. The mixture was refluxed under a nitrogen atmosphere for 5 h. The supernatant liquid was separated from the precipitate by hot filtration. After removal of the solvent from the filtrate using a rotary evaporator at 80 °C, the residue was dissolved in diethyl ether. The solution was washed three times with dilute hydrochloric acid and three times with deionized water. It was dried over anhydrous sodium sulfate, and the solvent was subsequently removed on a rotary evaporator. The product was purified twice by recrystallization from 100 mL of an *n*-hexane/ethyl acetate (1:1) mixture. Yield 10 g (66% of theoretical), white powder, purity > 99% (TLC), $T_m = 60$ °C. Elemental analysis for $C_{39}H_{72}O_6$ (636.99 g mol^{-1}): C, 73.83; H, 12.05 wt %. Calcd: C, 73.54; H, 11.39 wt %. ^{1}H NMR ($CDCl_3$, δ/ppm): 1.27 [m, 44H,

(8) (a) Hickner, M. A.; Ghassemi, H.; Kim, Y. S.; Einsla, B. R.; McGrath, J. E. *Chem. Rev.* **2004**, *104*, 4587. (b) Haile, S. M. *Acta Mater.* **2003**, *51*, 5981. (c) Grot W. *Chem. Ing. Tech.* **1972**, *44*, 167.
(9) Beginn, U. *Prog. Polym. Sci.* **2003**, *28*, 1049.
(10) Beginn, U.; Sheiko, S. S.; Möller, M. *Macromol. Chem. Phys.* **2000**, *201*, 1008.
(11) (a) Beginn, U.; Zipp. G.; Mourran A.; Möller, M. *Adv. Mater.* **2000**, *12*, 513. (b) Beginn, U.; Zipp, G.; Möller, M. *Adv. Mater.* **2000**, *12*, 510.
(12) Beginn, U.; Keinath S.; Möller, M. *Macromol. Chem. Phys.* **1998**, *199*, 2379.
(13) Zhu, X.-M.; Tartsch, B.; Beginn, U.; Möller, M. *Chem. Eur. J.* **2004**, *10*, 3871.
(14) Mohamadi, F.; Richards, N. G. J.; Guida, W. C.; Liskamp, R.; Lipton, M.; Caulfield, C.; Chang, G.; Hendrickson, T.; Still, W. C. *J. Comput. Chem.* **1990**, *11*, 440.
(15) Ferguson, D. M.; Kollman, P. *J. Comput. Chem.* **1991**, *12*, 620.
(16) Ponder, J. W.; Richards, F. M. *J. Comput. Chem.* **1987**, *8*, 1016.

−(CH_2)$_7$−CH_2CH_2OH], 1.47 [m, 6H, −CH_2(CH_2)$_2$OPh], 1.56 (m, 6H, −CH_2CH_2OH), 1.77 (m, 6H, −CH_2CH_2OPh), 3.63 [t, ^3J(H,H) = 6.6 Hz, 6H, −CH_2OH], 3.94 [t, ^3J(H,H) = 6.4 Hz, 2H, −CH_2OPh in the 2 position], 3.96 [t, ^3J(H,H) = 6.4 Hz, 4H, −CH_2OPh in the 1 and 3 positions], 6.54 [d, ^3J(H,H) = 8.3 Hz, 2H, $H_{aromatic}$ in the 4 and 6 positions], 6.91 [t, ^3J(H,H) = 8.3 Hz, 1H, $H_{aromatic}$ in the 5 position). ^{13}C NMR (CDCl$_3$, δ/ppm): 25.769 (−CH_2CH$_2$CH$_2$OH), 26.118 (−CH_2CH$_2$CH$_2$OPh), 29.65−30.40 (alkyl), 32.805 (−CH_2CH$_2$OH), 63.053 (−CH_2OH), 69.070 (−CH_2OPh in the 1 and 3 positions), 73.369 (−CH_2OPh in the 2 position), 106.758 ($C_{aromatic}$ in the 4 and 6 positions), 123.145 ($C_{aromatic}$ in the 5 position), 138.384 ($C_{aromatic}$ in the 2 position), 153.411 ($C_{aromatic}$ in the 1 and 3 positions).

1,2,3-Tris(11′-methacryloyl-undecyl-1′-oxy)benzene (2). In a 100-mL three-neck round-bottom flask equipped with a nitrogen inlet, 2.0 g (3.14 mmol) of compound **1**, 1.7 mL (12.3 mmol) of triethylamine, 50 mg (0.41 mmol) of 4-(dimethylamino)pyridine, and 10 mg (0.05 mmol) of 2,6-di-*tert*-butyl-4-methylphenol were dissolved in 15 mL of dried THF. The resulting solution was cooled with an ice/water mixture, and under intensive stirring, a solution of 1.2 mL (12.4 mmol) methacryloyl chloride was added dropwise. After complete addition, the solution was stirred at ambient temperature for 24 h. Subsequently, the solution was filtered, and the solvent was removed on a rotary evaporator. The residue was dissolved in 100 mL of diethyl ether. The solution was washed three times with a solution of 5 wt % sodium hydrogen carbonate in water, three times with dilute hydrochloric acid, and three times with a saturated solution of NaCl. The product was purified by column chromatography over silica gel, using *n*-hexane/ethyl acetate (8:1) as the mobile phase. Yield 1.64 g (62% of theoretical), transparent liquid, purity > 99% (TLC), T_m = 19.7 °C. Elemental analysis for $C_{51}H_{84}O_9$ (841.22 g mol^{-1}): C, 72.88; H, 10.06 wt %. Calcd: C, 72.82; H, 10.06 wt %. ^{1}H NMR (CDCl$_3$, δ/ppm): 1.30 [m, 44H, −(CH_2)$_7$−CH_2CH_2OPh], 1.47 [m, 6H, −CH_2(CH_2)$_2$OPh], 1.67 (m, 6H, −CH_2CH_2OMA), 1.77 (m, 6H, −CH_2CH_2OPh), 1.94 [s, 9H, CH_2=C(CH_3)−], 3.94 [t, ^3J(H,H) = 6.4 Hz, 6H, −CH_2OPh], 4.13 [t, ^3J(H,H) = 6.8 Hz, 6H, −CH_2OMA], 5.53 [m, 3H, −CH=C(CH$_3$)−, *E* to CH$_3$−], 6.09 [m, 3H, −CH=C(CH$_3$)−, *Z* to CH$_3$−], 6.53 [d, ^3J(H,H) = 8.3 Hz, 2H, $H_{aromatic}$ in the 4 and 6 positions], 6.89 [t, ^3J(H,H) = 8.3 Hz, 1H, $H_{aromatic}$ in the 5 position]. ^{13}C NMR (CDCl$_3$, δ/ppm): 18.285 [CH$_2$=C(*C*H$_3$)-], 25.965 (−CH_2CH$_2$CH$_2$OMA and −CH_2CH$_2$CH$_2$OPh), 28.55−30.40 (alkyl), 64.718 (−CH_2OMA), 68.944 (−CH_2OPh in the 1 and 3 positions), 73.224 (−CH_2OPh in the 2 position), 106.687 ($C_{aromatic}$ in the 4 and 6 positions), 123.101 ($C_{aromatic}$ in the 5 position), 125.039 [*C*H$_2$=C(CH$_3$)−], 136.485 [CH$_2$=*C*(CH$_3$)−], 138.321 ($C_{aromatic}$ in the 2 position), 153.349 ($C_{aromatic}$ in the 1 and 3 positions), 167.330 (−*C*OO−).

Sodium 2,3,4-Tris(11′-methacryloylundecyl-1′-oxy)benzenesulfonate (3). Under intensive stirring, 1 mL of concentrated sulfuric acid (95−97%) was added at ambient temperature to a well-stirred solution of 1.0 g (1.19 mmol) of **2** in 10 mL of chloroform. The resulting mixture was stirred for 5 min; afterward, it was poured into 100 mL of a saturated solution of NaCl containing 1.0 g of NaOH. The aqueous solution was adjusted to pH 7 and extracted with chloroform (three times with 50 mL each). After the organic phase had been dried over sodium sulfate, the solvent was evaporated. The product was purified by gradient column chromatography in ethyl acetate/ethanol. First, ethyl acetate was used to wash away organic impurities; subsequently, the product was washed out using a mixture of ethyl acetate and ethanol (1:5). Yield 0.83 g (74% of theoretical), waxy material, purity > 99% (^{1}H NMR). Elemental analysis for $C_{51}H_{83}O_{12}SNa$ (943.26 g mol^{-1}): C, 64.89; H, 9.15; S, 3.41; Na, 2.17 wt %. Calcd: C, 64.94; H, 8.87; S, 3.40; Na, 2.44 wt %. ^{1}H NMR (DMSO-d_6, δ/ppm): 1.27 [m, 44H, −(CH_2)$_7$−CH_2CH_2OPh], 1.41 [m, 6H, −CH_2(CH_2)$_2$OPh], 1.59 (m, 6H, −CH_2CH_2OMA), 1.67 (m, 6H, −CH_2CH_2OPh), 1.86 [s, 9H, CH$_2$=C(CH_3)−], 3.83 [t, ^3J(H,H) = 6.0 Hz, 2H, −CH_2OPh in the 3 position], 3.94 (m, 4H, −CH_2OPh in the 2 and 4 positions), 4.06 [t, ^3J(H,H) = 6.8 Hz, 6H, −CH_2OMA], 5.64 [m, 3H, −CH=C(CH$_3$)−, *E* to CH$_3$−], 6.00 [m, 3H, −CH=C(CH$_3$)−, *Z* to CH$_3$−], 6.63 [d, ^3J(H,H) = 8.8 Hz, 1H, $H_{aromatic}$ in the 5 position], 7.35 [d, ^3J(H,H) = 8.7 Hz, 1H, $H_{aromatic}$ in the 6 position). ^{13}C NMR (DMSO-d_6, δ/ppm): 17.896 [CH$_2$=C(*C*H$_3$)−], 25.419 (−CH_2CH$_2$CH$_2$OMA), 25,511, 25.676 (−CH_2CH$_2$CH$_2$OPh), 28.00−29.90 (alkyl), 64.172 (−CH_2OMA), 72.559 (−CH_2OPh in the 2 position), 73.156 (−CH_2OPh in the 4 position), 78.483 (−CH_2OPh in the 3 position), 106.563 ($C_{aromatic}$ in the 5 position), 122.739 ($C_{aromatic}$ in the 6 position), 125.320 [*C*H$_2$=C(CH$_3$)−], 134.616 ($C_{aromatic}$ in the 1 position), 135.920 [CH$_2$=*C*(CH$_3$)−], 147.744 ($C_{aromatic}$ in the 3 position), 150.268 ($C_{aromatic}$ in the 2 position), 153.474 ($C_{aromatic}$ in the 4 position), 166.435 (−*C*OO−).

2,3,4-Tris(11′-methacryloylundecyl-1′-oxy)benzenesulfonic Acid (4). **3** (0.1 g, 0.11 mmol) was dissolved in 10 mL of dried diisopropyl ether. The resulting solution was shaken overnight with 1 g of ion-exchange resin Amberlyst 15. Then, the ion-exchange resin was filtered off, and the solvent was removed under reduced pressure. The product was dried in a vacuum at 40 °C. Yield 0.097 g (99% of theoretical), colorless liquid, purity > 99% (TLC). Elemental analysis for $C_{51}H_{84}O_{12}S$ (921.28 g mol^{-1}): C, 63.00; H, 9.26 wt %. Calcd: C, 66.49; H, 9.19 wt %. ^{1}H NMR (CDCl$_3$, δ/ppm): 1.30 [m, 44H, −(CH_2)$_7$−CH_2CH_2OPh], 1.46 [m, 6H, −CH_2(CH_2)$_2$OPh], 1.66 (m, 6H, −CH_2CH_2OMA), 1.82 (m, 6H, −CH_2CH_2OPh), 1.94 [s, 9H, CH$_2$=C(CH_3)−], 3.96 [tt, ^3J(H,H) = 6.4 Hz, 4H, −CH_2OPh in the 3 and 4 positions), 4.13 [t, ^3J(H,H) = 6.4 Hz, 6H, −CH_2OMA], 4.18 [t, ^3J(H,H) = 7.2 Hz, 2H, −CH_2OPh in the 2 position], 5.54 [m, 3H, −CH=C(CH$_3$)−, *E* to CH$_3$−], 6.09 [m, 3H, −CH=C(CH$_3$)−, *Z* to CH$_3$−], 6.61 [d, ^3J(H,H) = 8.7 Hz, 1H, $H_{aromatic}$ in the 5 position], 7.52 [d, ^3J(H,H) = 8.7 Hz, 1H, $H_{aromatic}$ in the 6 position]. ^{13}C NMR (CDCl$_3$, δ/ppm): 18.326 [CH$_2$=C(*C*H$_3$)−], 25.950, 25.996, 26.051, 26.106 (−CH_2CH$_2$CH$_2$OMA and −CH_2CH$_2$CH$_2$OPh), 28.60−30.40 (alkyl), 64.869 (−CH_2OMA), 68.883 (−CH_2OPh in the 2 position), 73.797 (−CH_2OPh in the 4 position), 75.120 (−CH_2OPh in the 3 position), 106.847 ($C_{aromatic}$ in the 5 position), 125.254 [*C*H$_2$=C(CH$_3$)−], 126.338 ($C_{aromatic}$ in the 6 position), 136.470 ($C_{aromatic}$ in the 1 position), 136.497 [CH$_2$=*C*(CH$_3$)−], 142.137 ($C_{aromatic}$ in the 3 position), 150.753 ($C_{aromatic}$ in the 2 position), 157.110 ($C_{aromatic}$ in the 4 position), 167.636 (−*C*OO−).

Polymerization of 3 in the Mesophase. A thin film of **3** with 0.5% of 2,2-dimethoxy-2-phenylacetophenone (photoinitiator) was sandwiched into the gap between two glass slides connected with a 100-μm spacer. Photopolymerization was carried out by irradiation with an 8-W UV lamp at 366 nm for 12 h at room temperature. The film was released from the glass slide using sonication after immersion into water.

Results and Discussion

The synthesis of sodium 2,3,4-tris(11′-methacryloylundecyl-1′-oxy)benzenesulfonate (**3**) and the corresponding sulfonic acid (**4**) was carried out as depicted in Scheme 1. Pyrogallol was alkylated in cyclohexanone in the presence of anhydrous potassium carbonate with 11-bromo-1-undecanol to yield 1,2,3-tris(11′-hydroxyundecyl-1′-oxy)benzene (**1**) under reflux conditions. The product was purified by recrystallization from a mixture of *n*-hexane and ethyl acetate. The three hydroxy groups of **1** were subsequently reacted

Scheme 1. Synthesis of Sodium 2,3,4-Tris(11′-methacryloylundecyl-1′-oxy)benzenesulfonate (3) and 2,3,4-Tris(11′-methacryloylundecyl-1′-oxy)benzenesulfonic Acid (4)

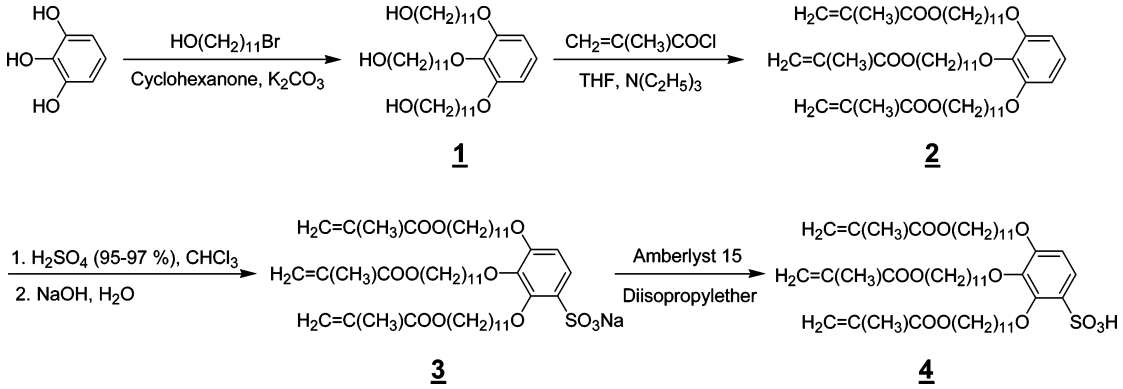

with methacryloyl chloride to yield the triester **2**. The sulfonation of **2** was carried out under very mild reaction conditions to avoid damage of the methacrylate groups. Concentrated sulfuric acid (95−97%) was added to a stirred solution of **2** in chloroform at room temperature. After conversion of the educt (ca. 5 min at 20 °C), the product was neutralized to sodium sulfonate **3** using an aqueous sodium hydroxide solution.

The sodium salt **3** was almost qualitatively transformed into the corresponding 2,3,4-tris(11′-methacryloyl-undecyl-1′-oxy)benzenesulfonic acid (**4**) by shaking a diisopropyl ether solution of **3** with Amberlyst 15 in its acid form. All intermediate and final products were characterized by means of ^{1}H and ^{13}C NMR spectroscopies, and their purity was checked by thin-layer chromatography and elemental analysis.

At ambient temperature, sodium sulfonate **3** is a waxy white material, whereas the corresponding sulfonic acid **4** is a viscous colorless liquid. The thermal behavior of these compounds was studied by means of polarizing optical microscopy (POM) and differential scanning calorimetry (DSC).

The DSC curves of final products **3** and **4** are shown in Figure 1, and Table 1 summarizes the observed phase-transition temperatures and enthalpies of these compounds. At the measurement conditions (10 °C min^{-1}), the phase transition of **3** was not fully reversible. In the second heating run, the transition temperature was lower, and the transition

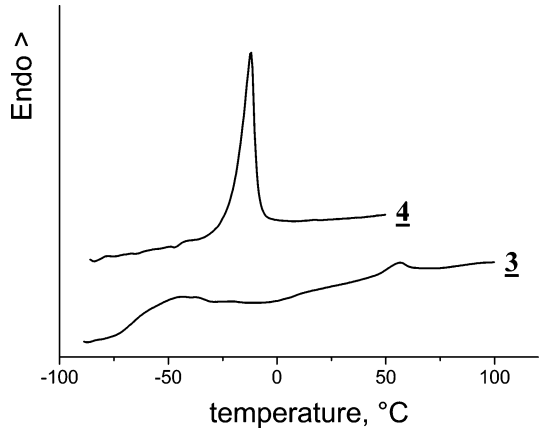

Figure 1. DSC traces of compounds 3 and **4**. Heating rate 10 °C/min, second heating run.

Table 1. Phase Transitions of Compounds 3 and 4

compd	phase transition[a]	T (°C)	ΔH (kJ mol^{-1})
3	glass transition	−63	
	clearing (M → I)	57	1.2
4	melting (C → I)	−12	26.5

[a] C = crystalline phase, M = mesophase, I = isotropic phase.

enthalpy was much smaller than those of the first heating run, indicating an incomplete phase transition upon cooling, most probably because of the high melt viscosity and low rate of mesophase formation. If the sample was kept at 4 °C for 24 h or annealed at 50 °C for 2 h after the first heating, the transition enthalpy again became comparable to that of the first heating run. The DSC trace of **3** obtained after annealing at 4 °C for 24 h is shown in Figure 1, where one can see an endothermal peak with a maximum at 57 °C and a very small transition enthalpy. At this temperature, POM showed a transition from a viscous birefringent phase to an optical isotropic phase. These results are indicative of the clearing transition of a liquid crystal. No typical liquid-crystalline texture was observed, probably because of high melt viscosity. Compound **3** did not crystallize on cooling until −100 °C; however, it vitrified at −63 °C. Thus, the mesophase formed by **3** can be frozen in the glass state.

According to the DSC measurements, the corresponding sulfonic acid **4** does not form any mesophases; instead, it crystallizes at low temperature. The large transition enthalpy of 26.5 kJ·mol^{-1} (Figure 1) can be related to a melting process to a crystalline phase. The reason for the crystallization instead of mesophase formation can be related to intramolecular hydrogen bonding, which leads to a decrease of amphiphilicity. Note that this behavior is similar to that of 2,3,4-tris(alkoxy)benzoic acids, which also fail to produce mesomorphic states.[17] Although this compound does not form any mesophases, it is a very useful intermediate for the preparation of different sulfonates, as well as complexes with polymer bases.

Small-angle X-ray scattering (SAXS) analysis was used to identify the structure of the mesophase formed by sodium sulfonate **3**. The SAXS data (Figure 2) are indicative of a hexagonal disordered columnar mesophase (Col_{hd}).[18] At room

(17) Levelut, A. M.; Malthete, J.; Destrade, C.; Tin, N.-H. *Liq. Cryst.* **1987**, *2*, 877.
(18) Pershan, P. S. *Structure of Liquid Crystal Phases*; World Scientific: Singapore, 1988.

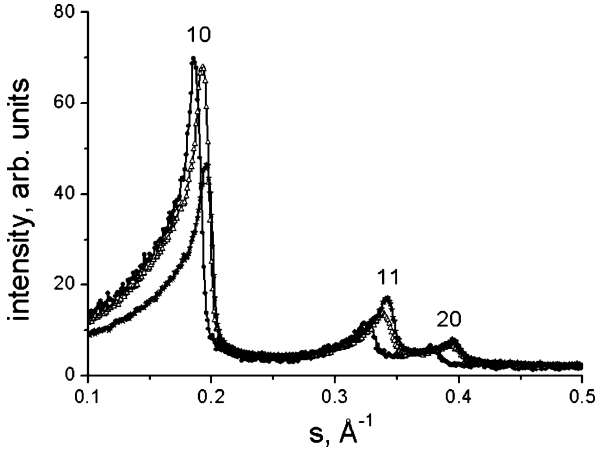

Figure 2. SAXS data for sodium sulfonate **3** at 20 (●), 53 (△), and 100 °C (★). Three reflections of the Col_{hd} phase are shown.

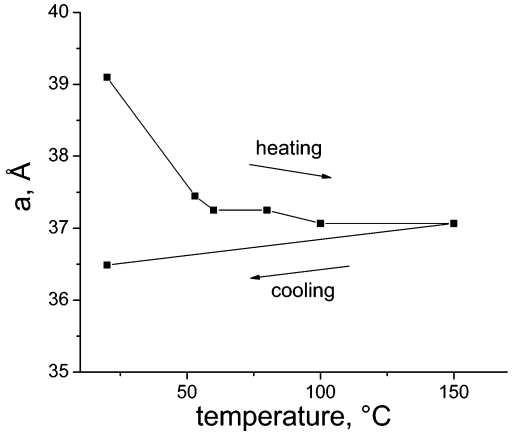

Figure 3. Temperature dependence of column diameter (*a*) for the Col_{hd} phase.

temperature, three distinct peaks—the strongest at $s = (0.186 \pm 0.001)$ Å^{-1} and two others at $s = 0.325$ and 0.379 Å^{-1}—were observed. The ratio of the measured *d* spacings ($d_0 = 33.9$ Å, $d_1 = 19.3$ Å, and $d_2 = 16.6$ Å) was found to be $1:1/\sqrt{3}:1/2$, and these reflections were attributed to the 10, 11, and 20 reflections of a two-dimensional hexagonal lattice with a lattice constant of $a = (39.1 \pm 0.2)$ Å.

As can be seen in Figure 2, heating to the melting temperature of **3** resulted in a significant shift of all observed peaks to wider angles, along with a change in the intensity distribution. The column diameter gradually decreased from 39.1 to 37.3 Å (Figure 3). Such marked changes in *d* spacing were observed earlier for similar columnar mesophases. The negative coefficient of thermal "expansion", $\beta = -(1.2-1.3) \times 10^{-3}$ K^{-1} was very close to the values obtained before [$-(1-2) \times 10^{-3}$ K^{-1}].[19] Surprisingly, above 57 °C, the SAXS curve contained the same three peaks corresponding to hexagonal columnar phases (Figure 2). The peaks shifted to the wider-angle area with temperature; however, the slope of the $a(T)$ dependence decreased strongly to the value of $\beta = -(5.5-9.0) \times 10^{-5}$ K^{-1}, which is common for solids (Figure 3). At the same time, the intensity of the 10 reflection became much weaker, whereas the 11 reflection intensified because of a redistribution of the electron density

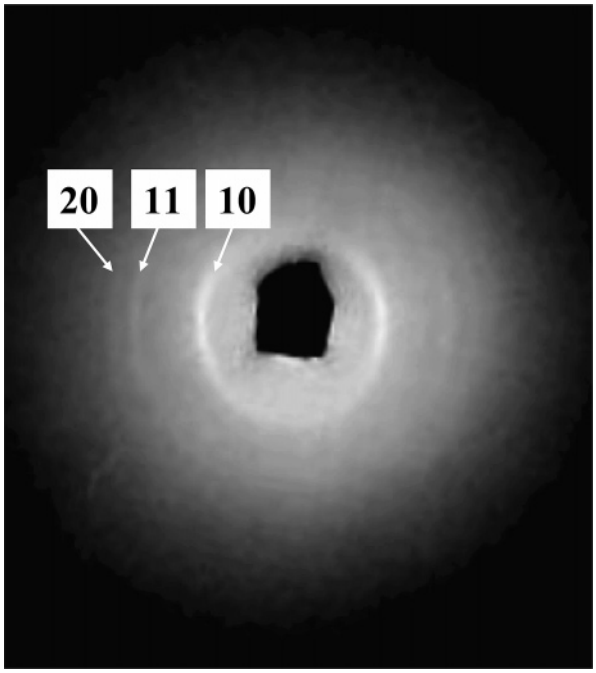

Figure 4. Two-dimensional SAXS pattern of an oriented fiber of **3**. The fiber is vertical. Three observed reflections and the absence of layer lines verify the hexagonal disordered columnar mesophase.

inside the columns. It is important to note that the experiment was carried out for sodium sulfonate **3** with an inhibitor added (0.2 wt % of 2,6-di-*tert*-butyl-4-methylphenol in **3**). Explanation for the maintenance of the columnar mesophase is a chemical cross-linking reaction occurring upon melting during the SAXS measurements. This was confirmed by the insolubility of the studied sample in chloroform after SAXS analysis. The apparent discrepancy in the SAXS, DSC, and POM results can be explained by the different experimental conditions. X-ray irradiation with continuous heating for several hours certainly caused the cross-linking reaction.

It is important to mention that uniaxial fibers can be drawn from the melt at the temperature above 60 °C with subsequent quenching to ambient temperature. The X-ray pattern of a fiber is shown in Figure 4. Three reflections were observed forming arcs only along the equatorial direction, indicating the presence of a two-dimensional hexagonal lattice. The value of $a = 36.7$ Å corresponds to the diameter of a cross-linked system (Figure 4). It highlights the opportunity to prepare the polymer fibers containing oriented functional ion-selective channels.

The number of molecules, N_{EC}, present in the hexagonal elementary cell per average height *h* of a Col_{hd} phase can be calculated from the macroscopic density ρ and the lattice constant *a* using the following equation[20,21]

$$\frac{N_{EC}}{h} = \frac{\sqrt{3}}{2} N_A \frac{\rho a^2}{M}$$

Here, *M* denotes the molecular weight of **3** ($M = 0.9426$

(19) Chvalun, S. N.; Shcherbina, M. A.; Bykova, I. V.; Blackwell, J.; Percec, V.; Kwon, Y. K.; Cho, J. D. *Polym. Sci. A* **2001**, *43*, 33.

(20) Percec, V.; Johansson, G.; Heck, J.; Ungar, G.; Batty, S. *J. Chem. Soc., Perkin Trans. 1* **1993**, 1411.

(21) Safinya, C. R.; Liang, K. S.; Varady, N. A.; Clark, N. A.; Anderson, G. *Phys. Rev. Lett.* **1984**, *53*, 1172.

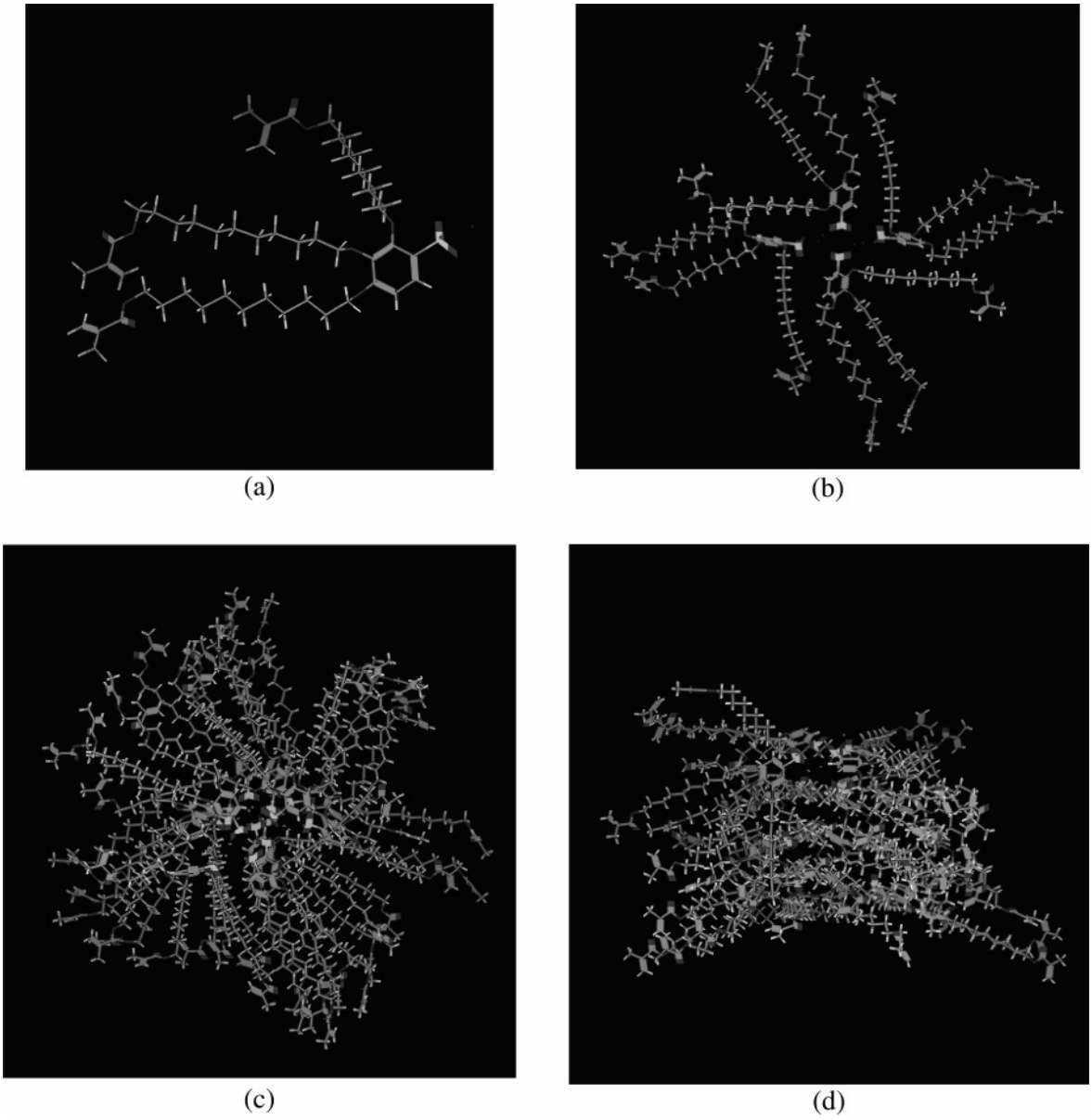

Figure 5. Molecular arrangement of 3 calculated by molecular modeling: (a) monomer, (b) top view of a tetramer, (c) top view of a 16-mer, (d) side view of a 16-mer.

kg/mol) and N_A is Avogadro's number. The density ρ of **3** was estimated by a flotation experiment in aqueous solutions of potassium iodide to be (1078 ± 5) kg·m^{-3}. The calculations gave the value about (0.907 ± 0.004) molecules/Å, which is in the range of values characteristic for gallic acid based species forming different types of columnar phases (0.63−1.3 molecules/Å).[22,23]

The height *h* of the average two-dimensional elementary cell was estimated by molecular modeling to be (5.5 ± 0.5) Å (Figure 5c), which is larger than the average spacing between adjacent benzene rings in the direction of the columnar axis as reported in the literature (3.74 Å).[21] This difference is most probably caused by the presence of the bulky sulfonate group in the molecule of **3**. Judging from the values obtained from molecular modeling, N_{EC} is (5.0 ± 0.4). Within the frame of the experimental error, it is justified to state that the columnar cross section is composed of four molecules of **3**. Corresponding to this value, the height *h* was calculated to be 4.4 Å. A more appropriate number of molecules per layer of the two-dimensional hexagonal lattice is six, which corresponds to *h* equaling 6.6 Å.

To derive a conclusion on the possible molecular arrangement within the mesophase, force-field-based molecular modeling calculations were performed. The calculated structures of an isolated molecule, a tetramer, and a 16-mer of **3** are depicted in Figure 5.

Molecular modeling showed that the sodium cation in the monomer of **3** faces the sulfonate group, positioned approximately on the extension of the C−S bond (cf. Figure 5a). Four molecules, prearranged to form a planar "end-to-end" aggregate with a hydrophilic center and a hydrophobic rim, remained in this structure when the force-field energy optimization was performed. In this "tetramer cross section", the four sodium cations remain in close proximity of the

(22) Percec, V.; Johansson, G.; Ungar, G.; Zhou, J. *J. Am. Chem. Soc.* **1996**, *118*, 9855.
(23) Kwon, Y. K.; Chvalun, S.; Schneider A.-I.; Blackwell, J.; Percec, V.; Heck, J. A. *Macromolecules* **1994**, *27*, 6129.

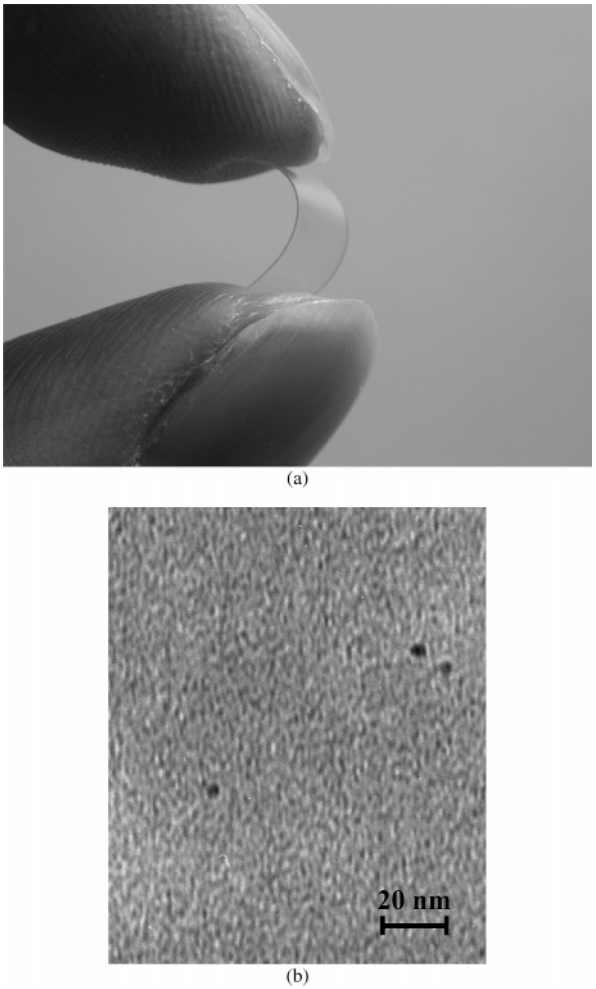

Figure 6. (a) Photo of the film prepared by polymerization of 3 in the mesomorphous state. (b) Transmission electron micrograph of the thin flim.

sulfonate headgroups, positioned at almost equal distance to two neighboring sulfonate anions. Two of the cations are located above the plane of the disk, whereas the other two sodium ions are arranged below this plane (Figure 5b). This flat aggregate was used as the structural unit to build up a cylinder. Four "cross section aggregates" were stacked and subsequently optimized with respect to the force-field energy; the resulting structure is shown in Figure 5c (top view) and 5d (side view).

In Figure 5c, one can see clearly that, in the center of the cylinder, a potential ion channel is formed. The position of the cations is mainly between the tetramer cross sections, but their arrangement is not highly periodic and regular as within a crystalline structure. Local changes of the conformation of the alkyl chains and subsequent energy optimization of the 16-mer caused variations in the position of the center of gravity of the treated molecule that also changed the positions of the cations in the vicinity of that molecule.

The calculated diameter of the cylinder was approximately 50 Å, exceeding the measured lattice parameter $a = 39.1$ Å by 22%. One possible explanation for this difference is that the molecular modeling calculation was carried out for an isolated column in vacuo. In a liquid-crystalline phase, the environment of the molecules is of higher density; hence, the dense packing of the columns may impede the formation of fully stretched alkyl chain conformations and limit the column diameter to the measured size. Another possibility is that the molecule surfaces are tilted relative to the columnar axis as described previously for the wedge-shaped amphiphlic molecules.[19,20,23−25] It is also possible that interdigitation, i.e., partial overlap and interpenetration of neighboring columns, reduces the distance between the centers of the columns. Neither the force-field calculations nor the measured SAXS data allow these three possibilities to be distinguished.

Thin solid films of **3** were prepared by UV-initiated polymerization in the mesophase at room temperature. The films were turbid, and almost no change of the optical texture was observed during the course of polymerization. After polymerization, heating did not lead to the disappearance of the birefringence. Hence, the columnar mesophase structure was permanently fixed in the cross-linked state. The films obtained from polymerized pure **3** were flexible and could be bent without breaking or forming visible cracks (Figure 6a).

Transmission electron microscopy (TEM) was utilized to analyze the structure of the thin film of polymerized **3**. The TEM micrograph (Figure 6b) clearly shows a columnar structure with a column diameter (3.0 ± 1.0) nm. This value is slightly smaller than that derived from the SAXS data of **3**. However, it is a common phenomenon that the characteristic dimensions in monomer systems shrink upon polymerization.

Summary

In this work, the synthesis of polymerization-active liquid-crystalline sodium 2,3,4-tris(11′-methacryloylundecyl-1′-oxy)benzene sulfonate (**3**) is described. Compound **3** forms a disordered hexagonal columnar mesophase with the sulfonate groups confined to the center of the columns, thus preforming a potential ion channel. Photopolymerization of thin films of **3** in the mesophase yielded free-standing, solid but flexible films containing sulfonate stacks in a permanently arrested state.

Measurement of the ion-transport characteristics of polymerized films of **3** such as ion permeability and cation/anion and cation/cation selectivity is in progress and will be reported in an upcoming work.

Acknowledgment. The financial support of the BMBF (funding no. 03 D 0047 5) and the German Research Foundation DFG (SFB 569) is gratefully acknowledged. X.Z. thanks the Alexander von Humboldt foundation for financial support. A.V.B. and M.A.S. thank the Russian Foundation for Basic Research for financial support (funding no. 05-03-32904).

CM060305Y

(24) Johansson, G.; Percec, V.; Ungar, G.; Abramic, D. *J. Chem. Soc., Perkin Trans. 1* **1994**, 447.
(25) Percec, V.; Heck, J.; Tomazos, D.; Falkenberg, F.; Blackwell, H.; Ungar, G. *J. Chem. Soc., Perkin Trans. 1* **1993**, 2799.